Journal of Dental Sciences 21 (2026) 282–293

Available online at www.sciencedirect.com

ScienceDirect

journal homepage: www.e-jds.com

Original Article

Ovatodiolide overcomes cisplatin resistance in head and neck cancer by disrupting a novel oncogenic signature and cancer-associated fibroblast activation

Chi-Hsueh Yang [a†], Rachel Raditya Renantha [b†], Po-Chih Hsu [c,d], Alexander TH. Wu [b,e,f,g], Szu-Yuan Wu [h,i], Nur Azizah [j,k], Ritmaleni Ritmaleni [j,k], Jia-Hong Chen [l], Jih-Chin Lee [m], Chih-Yuan Fang [n,o], Kuan-Chou Lin [n,o*]

[a] *Department of Dentistry, Lotung Poh-Ai Hospital, Yilan, Taiwan*
[b] *International Master Program in Translational Science, College of Medical Science and Technology, Taipei Medical University, New Taipei City, Taiwan*
[c] *Department of Dentistry, Taipei Tzu Chi Hospital, New Taipei City, Taiwan*
[d] *Institute of Oral Medicine and Materials, College of Medicine, Tzu Chi University, Hualien, Taiwan*
[e] *Clinical Research Center, Taipei Medical University Hospital, Taipei Medical University, Taipei, Taiwan*
[f] *Graduate Institute of Medical Sciences, National Defense Medical Center, Taipei, Taiwan*
[g] *Taipei Heart Institute, Taipei Medical University, Taipei, Taiwan*
[h] *Big Data Center, Lotung Poh-Ai Hospital, Yilan, Taiwan*
[i] *Division of Radiation Oncology, Lotung Poh-Ai Hospital, Yilan, Taiwan*
[j] *Department of Pharmaceutical Chemistry, Faculty of Pharmacy, Universitas Gadjah Mada, Yogyakarta, Indonesia*
[k] *Curcumin Research Center, Faculty of Pharmacy, Universitas Gadjah Mada, Yogyakarta, Indonesia*
[l] *Division of Hematology/Oncology, Department of Medicine, Tri-Service General Hospital, National Defense Medical Center, Taipei, Taiwan*
[m] *Department of Otolaryngology, Head and Neck Surgery, Tri-Service General Hospital, National Defense Medical Center, Taipei, Taiwan*
[n] *School of Dentistry, College of Oral Medicine, Taipei Medical University, Taipei, Taiwan*
[o] *Department of Oral and Maxillofacial Surgery, Wan Fang Hospital, Taipei Medical University, Taipei, Taiwan*

Received 31 July 2025; Final revision received 25 August 2025
Available online 8 September 2025

* Corresponding author. Department of Oral and Maxillofacial Surgery, Wan Fang Hospital, Taipei Medical University, No. 111, Sec. 3, Xinglong Rd., Wenshan Dist., Taipei 116081, Taiwan.
E-mail address: kclin0628@tmu.edu.tw (K.-C. Lin).
† These two authors contributed equally to this study.

https://doi.org/10.1016/j.jds.2025.08.041

KEYWORDS
Head and neck squamous cell carcinoma;
Cisplatin resistance;
SIS signature;
Cancer-associated fibroblasts;
Ovatodiolide

Abstract *Background/purpose:* Malignant head and neck squamous cell carcinoma (HNSCC) is an aggressive cancer with complex tumor microenvironment interactions. We aimed to identify key molecular drivers and therapeutic targets using bioinformatics approaches and examine their associations with cancer-associated fibroblasts (CAF).
Materials and methods: We analyzed three HNSCC transcriptomic datasets using bioinformatics. Protein–protein interaction networks were created using STRING, and pathway enrichment was also performed. The clinical relevance and CAF association of genes were evaluated using the TCGA HNSCC cohort and TIMER 2.0. Molecular docking predicted ovatodiolide binding to target proteins. Bioinformatics findings were validated in HNSCC cell lines and normal fibroblasts (WS1) by assessing cell viability, tumor spheroid formation, and CAF transformation through viability assays, qPCR, and Western blot. A mouse model of cisplatin resistance was used to test ovatodiolide's therapeutic effect.
Results: Our bioinformatics identified a nine-gene oncogenic network in HNSCC enriched in inflammatory and profibrotic pathways. A core three-gene SIS oncogenic signature (SERPINE1, INHBA, SPP1) was identified. High SIS expression correlated with poor survival and increased CAF infiltration. Docking predicted favorable binding of ovatodiolide to SERPINE1, SPP1, and INHBA. CAF-conditioned medium enhanced the stemness and chemoresistance of HNSCC cells, promoting SIS signature and stemness markers. Ovatodiolide suppressed oncogenic properties and CAF activation, decreasing SIS and CAF markers. In a mouse model, ovatodiolide overcame cisplatin resistance by reducing the SIS signature.
Conclusion: The SIS signature contributes to HNSCC progression, stemness, and drug resistance by facilitating CAF generation. Ovatodiolide disrupts this signature and inhibits CAF transformation.

Introduction

Head and neck squamous cell carcinoma (HNSCC) encompasses a diverse group of malignancies that arise from the mucosal lining of the oral cavity, pharynx, and larynx.[1,2] HNSCC poses a significant global health challenge. Taiwan is noted for having one of the highest incidence rates of HNSCC in the world, particularly for oral and pharyngeal cancers. According to statistics from the Taiwan Cancer Registry 2021, invasive cancers of the oral cavity, oropharynx, and hypopharynx ranked as the third most common cancer among Taiwanese males, with an age-adjusted incidence rate of 40.94 per 100,000. Despite advancements in treatment options, including surgery, radiotherapy, chemotherapy, and immunotherapy, many patients still face a poor prognosis due to the high rates of locoregional recurrence, distant metastasis, and ultimately the development of therapy resistance.[3] Therefore, understanding the mechanisms behind HNSCC's acquired or inherent resistance to therapies and identifying targetable biomarkers represents a critical research gap that must be urgently addressed.

Accumulated reports indicate that the complexity of HNSCC arises not only from genetic and epigenetic alterations within the tumor cells but also from interactions with the tumor microenvironment (TME).[4] The TME is a dynamic ecosystem comprising various stromal cells, immune cells, extracellular matrix components, and signaling molecules, all collectively influencing tumor initiation, progression, metastasis, and therapeutic response.[5] Among the key TME cellular constituents, cancer-associated fibroblasts (CAFs) are generally considered critical regulators of tumor behavior. CAFs are activated fibroblasts that contribute to matrix remodeling, secrete growth factors and cytokines, and modulate immune cell infiltration, creating a pro-tumorigenic and immunosuppressive niche. Insights into the shared molecular networks underlying HNSCC tumorigenesis and CAF transformation are key to developing strategies that simultaneously target both tumor cells and the TME.

Based on these premises, we employed a comprehensive bioinformatics approach, analyzing independent HNSCC transcriptomic datasets (GSE31056,[6] GSE23558,[7] GSE75538).[8] We then identified a novel oncogenic signature, the SIS signature (comprising SERPINE1, INHBA, and SPP1), which was consistently upregulated in HNSCC tumors and showed a significant correlation with poor overall survival and increased infiltration of cancer-associated fibroblasts (CAFs). These findings strongly suggest the SIS signature acts as a critical mediator connecting HNSCC cells with the pro-tumorigenic CAF-rich microenvironment.

Recognizing the potential of this novel SIS-CAF axis as a therapeutic target, we explored potential therapeutic strategies. Leveraging the vast potential of phytochemicals as lead compounds for new therapeutics, we focused on ovatodiolide. Ovatodiolide, a macrocyclic diterpenoid, was selected based on its documented anti-inflammatory and anti-cancer properties, including those previously demonstrated by our group in suppressing malignancy and modulating the TME.[9,10] Furthermore, molecular docking results indicated ovatodiolide's potential to interact with members of the SIS signature.

Building on these findings and rationale, we aim to clarify the precise role of the SIS signature in HNSCC tumorigenesis while confirming its functional interaction with CAFs. We evaluated ovatodiolide's therapeutic potential in disrupting this crucial SIS-CAF axis, both in vitro and in vivo. More importantly, we demonstrated its ability to overcome cisplatin resistance. Our results indicate that the SIS signature serves as a vital link between HNSCC cells and CAFs, promoting cancer stemness and cisplatin resistance. Ovatodiolide can effectively disrupt this link, presenting a promising therapeutic strategy for addressing drug-resistant HNSCC.

Materials and methods

Identification of oncogenic signature for head and neck cancer

The transcriptomic head and neck cancer datasets: GSE31056,[6] GSE23558,[7] and GSE75538,[8] were retrieved from the publicly available Gene Expression Omnibus (GEO) database.[11] The samples were categorized into tumor and normal samples and were then subjected to analysis using GEO2R tools. The parameters were set as log2 fold change (FC) threshold of 1.5, level of cutoff 0.05, and Benjamin & Hochberg for *P* adjustment. The upregulated DEGSs were downloaded and analyzed using Excel. The overlapped genes between the datasets were analyzed and visualized using jvenn.[12] The protein−protein interactions among the identified upregulated overlapped genes were evaluated using the STRING database.[13] Furthermore, the pathways enriched were also investigated based on the Wikipathway enrichment pathways. Among the nine identified DEGs, three genes: SERPINE1, INHBA, and SPP1, were selected for further evaluation.

SERPINE1, INHBA, SPP1 (SIS) expression, overall survival (OS), and cancer-associated fibroblasts (CAFs) infiltration analysis

The upregulated SIS signatures level was supported by the results from GEPIA2.0 database[14] search accessed on October 14, 2024. The parameters used both TCGA and GTEx data and a cutoff of log2 fold change (FC) of 1.5. The expressions of the genes were visualized using a box plot. Furthermore, the head and neck cancer samples were divided into high and low SIS gene signature expressions, and the overall survival (OS) was estimated. The SIS expression in different molecular subtypes of head and neck cancer was evaluated using TISIDB database[15] and the TIMER2.0 database[16] was utilized to determine the association between the expression of SIS signatures and CAF infiltration. Due to the highest Rho values and a significant $P < 0.05$, the tumor immune dysfunction and exclusion (TIDE) method was chosen.

Molecular docking simulation of ovatodiolide and SERPINE1, INHBA, SPP1

The 3D protein structures of SERPINE1 (PDB ID: 1LJ5) and INHBA (PDB ID: 2ARV)[17] were retrieved from the Protein Data Bank. The FASTA sequence of SPP1 was obtained from Uniprot (ID: P10451).[18] The FASTA sequence was used as the input to generate the 3D protein structure using SWISSMODEL.[19] After generating the 3D structure, the heteroatoms and water molecules in the proteins were removed using Discovery Studio Visualizer. Then, the PDB files of the proteins were converted to PDBQT files using Autodock.[20] Aside from the protein, the ligand, ovatodiolide, with a chemical structure obtained from PubChem (CID: 38347030), was converted to a PDB file using an online SMILES translator from NCI. Autodock was used to convert the PDB to a PDBQT file. The molecular docking of ovatodiolide and the SIS signature genes was performed using Command Prompt (Vina), and the interactions were visualized using BIOVIA Discovery Studio Visualizer 2024.

Cell lines and cell culture

Head and neck cancer cell lines (CAL27 and Ca9-22) and human skin fibroblast cells (WS1) were obtained from the American Type Culture Collection (ATCC, Manassas, VA, USA) and cultured according to the supplier's recommended conditions. The generation of tumor spheroids was performed following a previously established protocol with slight modifications.[21] In brief, CAL27 and Ca9-22 cells were seeded in ultra-low-attachment 6-well plates (Corning Inc., Taipei, Taiwan) at a concentration of 10,000 cells per well in DMEM/F12 medium (Gibco, CA, USA), supplemented with insulin, epidermal growth factor (20 ng/ml), basic fibroblast growth factor (10 ng/ml), N2, and B27 (Invitrogen, CA, USA), for 5 days. Only tumor spheroids with a diameter $\geq$200 μm were counted. The tumor-conditional medium (TCM) was collected from CAL27 and Ca9-22 spheroid culture. TCM was centrifuged at 300×*g* for 5 min, followed by another spin at 2000×*g* for 10 min to remove cell debris. The TCM was then filtered through a 0.22 μm filter to eliminate residual debris or apoptotic bodies further. This TCM was then used for WS1 transformation experiments.

Cell viability assays

To determine the IC50 of CAL-27 and Ca9-22 cells in 2D cell culture, the sulforhodamine B assay (SRB) was used. Ca9-22 and CAL-27 were seeded in 96-well plates at densities of 10^4 cells/well and 2 × 10^4 cells/well, respectively. The next day after seeding, the cells were treated with ovatodiolide. Following 48 h of incubation, the cell media was removed, washed with PBS once, and 100 μL of 10 % TCA was added to fix the cells. The plate was then incubated at 4 °C for at least 1 h or overnight. After the cells were fixed, the wells were washed once with ddH20, and 50 μL of 0.4 % SRB dye was added. The dye was left at room temperature in the dark for 30 min. Subsequently, the SRB dye was removed, the wells were rinsed three times with 1 % acetic acid, and left to air dry overnight at room temperature. Then, 10 mM of Tris buffer solution was added to each well to dissolve the stained cells. The plate was placed on a shaker for 15 min and then read in a microplate reader with an absorbance measurement at 540 nm. The absorbance values were then analyzed in Excel and GraphPad Prism 8.4.2. The cell viability of tumor spheroids was conducted

using ATPase activity assay (Blossom Biotechnologies Inc., Taipei, Taiwan), following the vendor's protocol.

Quantitative polymerase chain reaction (qPCR)

The CAL-27 and Ca9-22 cells were treated with ovatodiolide and then harvested. The total RNA from ovatodiolide-treated and control CAL-27 and Ca9-22 cells was isolated using the GENEzol™ TriRNA Pure Kit (Geneaid Biotech Ltd, New Taipei City, Taiwan) according to the manufacturer's guidelines. The total RNA was reverse transcribed into complementary DNA (cDNA), and quantitative PCR (qPCR) was performed using SYBR Green (Thermo Fisher Scientific Inc., Taipei, Taiwan). The data was analyzed and visualized using GraphPad Prism 8.4.2. The statistical method used was two-way ANOVA. The data presented in the bar graph indicates the mean and standard deviation (SD). An asterisk indicates the *P*, with *, **, *** indicating $P < 0.05$, $P \leq 0.01$, and $P \leq 0.001$, respectively. The primers are listed in Table 1.

Western blotting

Total protein lysates from HNSCC cell lines, including parental, tumor spheroids, and those from TCM coculture experiments, were purified and collected using a Total Protein Extraction Kit (Cat No. BC-K3011010, Blossom Biotechnologies Inc., Taipei, Taiwan) according to the manufacturer's protocol. A total of 10 μg of protein sample was dissolved in reducing sample buffer and added to each well. Protein samples were then separated with standard SDS-PAGE procedures (Bio-Rad, Hercules, CA, USA) and transferred onto a polyvinylidene difluoride (PVDF) membrane. The membranes were then blocked and incubated with primary antibodies. The following antibodies were used in this study: SERPINE1 (13801-1-AP, Proteintech, Rosemont, IL, USA), INHBA (17524-1-AP, Proteintech, Rosemont, IL, USA), SPP1 (ab63856, Abcam, Taipei, Taiwan), anti-MMP3 antibody (EP1186Y, Abcam, Taipei, Taiwan), YAP1 (13584-1-AP, Proteintech, Rosemont, IL, USA), anti-GAPDH antibody (ab9485, Abcam, Taipei, Taiwan), and HRP-conjugated goat anti-rabbit IgG (H + L) secondary antibody (SA00001-2, Proteintech, Rosemont, IL, USA).

Immunofluorescence imaging

WS1 and thereafter transformed CAFs were plated in six-well chamber slides (Nunc™, Thermo Fisher Scientific, Rochester, NY, USA) for 24 h. The immunofluorescence imaging experiment to examine the CAF markers was performed according to the vendor's protocol. Primary antibodies were then added and incubated at room temperature for 1 h. Antibodies used in these experiments include: vimentin (ab137321, Abcam, Cambridge, UK), α-SMA (ab7817, Abcam, Taipei, Taiwan), goat anti-rabbit IgG H&L (Alexa Fluor® 488) secondary antibody (ab150077, Abcam, Taipei, Taiwan), and goat anti-mouse IgG H&L (Alexa Fluor® 488) secondary antibody (ab150113, Abcam, Taipei, Taiwan). Stained cells were then imaged using a Zeiss Axiophot fluorescence microscope (Carl Zeiss, Oberkochen, Germany). Images were acquired with an AxioCam MRc digital camera and analyzed with AxioVision software (Carl Zeiss, Oberkochen, Germany).

In vivo evaluation of ovatodiolide's therapeutic potential

All in vivo experiments were strictly adhered to the Institutional Animal Care and Use Committee or Panel (IACUC/IACUP) of the National Defense Medical Center (Approval No.: IACUC-24-028). Six-week-old NOD/SCID mice (BioLASCO, Taipei, Taiwan), weighing approximately 20 g, were housed under specific pathogen-free conditions with a 12-h light/dark cycle, controlled temperature, and humidity, and had ad libitum access to clean food and water. Ca9-22 tumoroids containing cancer-associated fibroblasts (CAFs) (Cell number ratio, Ca9-22:WS1 = 5:1) were first established under 3D, serum-deprived conditions for 5 days, and harvested and dissociated into single-cell suspensions to establish the xenograft model. Cells were briefly washed in PBS, counted, and resuspended in a 1:1 mixture of PBS and Matrigel (Corning, Taiwan) at a concentration of

Table 1 Primer list for qPCR.

GENE	Forward	Reverse
SERPINE1	TTCAAGATTGATGACAAGGGC	CTCATCCTTGTTCCATGGC
INHBA	GCAGTCTGAAGACCACCCTC	ATGATCCAGTCATTCCAGCC
SPP1	CTCCATTGACTCGAACGACTC	CAGGTCTGCGAAACTTCTTAGAT
MMP1	AAGGCCAGTATGCACAGCTT	TGCTTGACCCTCAGAGACCT
MMP3	CGGTTCCGCCTGTCTCAAG	CGCCAAAAGTGCCTGTCTT
CD44	CCCAGATGGAGAAAGCTCTG	ACTTGGCTTTCTGTCCTCCA
YAP1	TAGCCCTGCGTAGCCAGTTA	TCATGCTTAGTCCACTGTCTGT
α-SMA	CTATGCCTCTGGACGCACAACT	CAGATCCAGACGCATGATGGCA
Vimentin	TGGCACGTCTTGACCTTGAA	GGTCATCGTGATGCTGAGAA
TGFβ1	CAACAATTCCTGGCGATACCTCA	GGTAGTGAACCCGTTGATGTCCA
GAPDH	CATCATCCCTGCCTCTACTG	GCCTGCTTCACCACCTTC

Abbreviations: SERPINE1: serpin family E member 1, INHBA: inhibin subunit beta A, SPP1: secreted phosphoprotein 1, MMP1: matrix metallopeptidase 1, MMP3: matrix metallopeptidase 3, YAP1: Yes1 associated transcriptional regulator, α-SMA: alpha smooth muscle actin, TGFβ1: transforming growth factor beta 1, GAPDH: glyceraldehyde-3-phosphate dehydrogenase. T: Thymine, C: cytosine, A: adenine, G: guanine.

1×10^6 cells per 100 μL. Each mouse was subcutaneously injected with 100 μL cell suspension (approximately 1×10^6 cells) into the right flank. Mice were monitored daily for general health and tumor development. Treatments began approximately two weeks post-injection, once tumors became palpable. Animals were randomly allocated to four groups (n = 5 per group): (1) Sham control, receiving vehicle (PBS, i.p., 5 times per week); (2) Cisplatin (CDDP) monotherapy, receiving CDDP (5 mg/kg, i.p., once weekly); (3) Ovatodiolide (OV) monotherapy, receiving OV (10 mg/kg, i.p., 5 times per week); and (4) Combination regimen, receiving CDDP (2.5 mg/kg, i.p., once weekly) and OV (10 mg/kg, i.p., 5 times per week). Tumor volume and body weight were measured weekly using an electronic caliper and scale, respectively. Tumor volume (V) was calculated as $V = (L \times W^2)/2$, where L is the longest diameter and W is the perpendicular diameter. At the end of the study, all mice were humanely euthanized. No tumors exceeded a volume of 1500 mm^3, and no mice showed significant body weight loss (>20 % of initial body weight) or other signs of distress under IACUC guidelines. Tumor tissues were collected for further analyses following euthanasia.

Results

Transcriptomic identification of an oncogenic signature for head and neck cancer

We employed a bioinformatics approach to identify novel molecular networks that contribute to the tumorigenic properties of HNSCC. First, we collected and analyzed three transcriptomic datasets from head and neck cancer patients (GSE31056, GSE23558, and GSE75538, Fig. 1A). We assessed the most significantly upregulated genes across the three datasets and identified nine commonly shared genes: MMP1, MMP3, MMP10, SPP1, INHBA, SERPINE1, IL24, CXCL10, and SCG5 (Fig. 1B). Subsequently, a STRING analysis of these nine genes revealed an oncogenic network in which SERPINE1, MMPs (1, 1,3, and 10), SPP1, CXCL10, and INHBA form a functional cluster, suggesting their strong associations (Fig. 1C). Gene set enrichment analysis (GSEA) indicates that these genes are significantly enriched in pathways involving proinflammatory and profibrotic mediators, matrix metalloproteinases, TGF-beta receptor signaling, and Oncostatin M signaling pathways (Fig. 1D). Collectively, our bioinformatics data strongly suggest that inflammation plays a key role in HNSCC tumorigenesis and that the members of this oncogenic/inflammatory network can potentially be therapeutic targets.

Elevated SERPINE1, INHBA, and SPP1 (SIS oncogenic signature) expressions correlate with poor prognosis in head and neck squamous cell carcinoma and a high infiltration level of cancer-associated fibroblasts (CAFs)

After establishing the nine-gene inflammatory/fibrotic signaling network, we narrowed it down to three genes, SERPINE1, INHBA, and SPP1 (the SIS oncogenic signature), based on their roles in tumorigenesis and association with

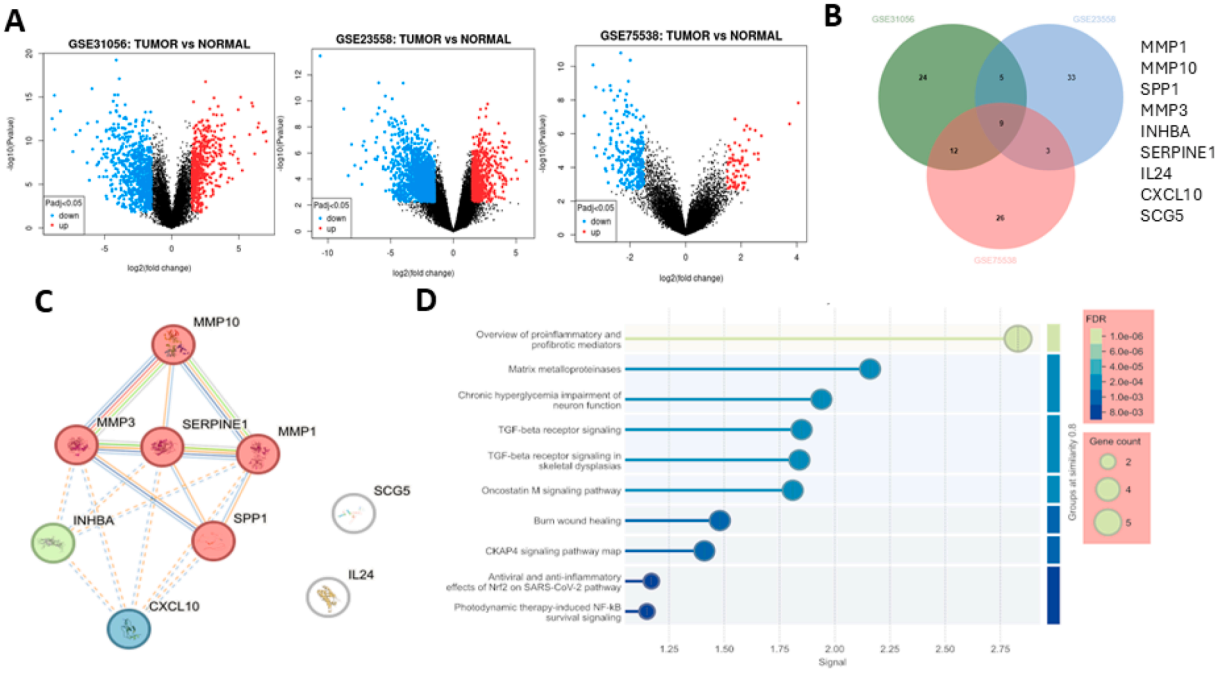

Figure 1 Transcriptomic identification of an oncogenic signature for head and neck cancer. (A) Workflow diagram showing analysis of three head and neck cancer datasets (GSE31056, GSE23558, GSE75538) from the GEO database. (B) Venn diagram displaying nine commonly upregulated genes (MMP1, MMP3, MMP10, SPP1, INHBA, SERPINE1, IL24, CXCL10, SCG5) across the three datasets. (C) STRING network analysis reveals functional clustering of the nine genes. (D) Gene set enrichment analysis showing enrichment in proinflammatory, profibrotic, matrix metalloproteinase, TGF-beta, and oncostatin M signaling pathways. GEO: Gene Expression Omnibus; STRING: Search Tool for the Retrieval of Interacting Genes/Proteins; TGF: transforming growth factor.

the tumor microenvironment (TME).[22–24] Gene expression analysis from the TCGA HNSCC database supports our notion that SERPINE1, INHBA, and SPP1 mRNA levels are significantly higher in tumor tissues compared to their normal counterparts (Fig. 2A). More importantly, patients with higher expression of the SIS oncogenic signature are significantly associated with a lower overall survival rate (Hazard ratio = 1.7; Logrank P = 6.9e-05, Fig. 2B). We further examined the expression profile of the SIS oncogenic signature, focusing on HNSCC molecular subtypes.[15] SPP1 expression is strongly associated with the classical and mesenchymal subtypes, INHBA is higher in the basal and mesenchymal subtypes, and SERPINE1 is elevated in basal, classical, and mesenchymal subtypes (Fig. 2C). The high expression level of the SIS oncogenic signature across the different subtypes of HNSCC suggests that this signature covers the heterogeneous nature of HNSCC. In addition, our findings from the TIMER 2.0 analytical tool.[16] Demonstrate that the SIS oncogenic signature expression significantly correlates with the level of tumor-infiltrating cancer-associated fibroblasts (CAFs) in the HNSCC TCGA database (Fig. 2D). INHBA expression shows the highest correlation with CAF infiltration (Rho = 0.642; P = 1.64e-58), followed by SERPINE1 (Rho = 0.583; P = 3.54e-46) and SPP1 (Rho = 0.339; P = 1.14e-14). Our findings indicate that an increased expression of the SIS oncogenic signature correlates with poor prognosis in HNSCC patients and a high level of tumor-infiltrating CAFs. The latter suggests a potential underlying factor for drug resistance and distant metastasis.

Molecular docking simulations predict stable binding of ovatodiolide to SERPINE1, INHBA, and SPP1

Following our pathway-level analyses that implicated the SIS oncogenic signature in inflammation, fibrosis, matrix remodeling, and TGF-β/Oncostatin M-driven CAF activation, we aimed to identify small-molecule disruptors of this signature. Ovatodiolide, a macrocyclic diterpenoid with documented anti-inflammatory and anti-cancer properties,[9,25] was docked in silico against the SIS oncogenic signature members, SERPINE1, SPP1, and INHBA, to evaluate its potential as a direct inhibitor. The docking simulations (Fig. 3) demonstrated favorable binding free energies (ΔG<0) for all three proteins, with the strongest predicted affinity for SERPINE1 (ΔG = −7.5 kcal/mol), followed by SPP1 (−6.5 kcal/mol) and INHBA (−6.4 kcal/mol). In the SERPINE1: ovatodiolide complex, the ligand (ovatodiolide) interacts with both hydrophobic residues (Val274, Leu273, Phe358, Pro379) and polar contacts (Ala239, Asp222), anchoring into the reactive-center loop region (Upper panel, Fig. 3). For SPP1, two hydrogen bonds to Arg159 and Gly160 secure the lactone core, while

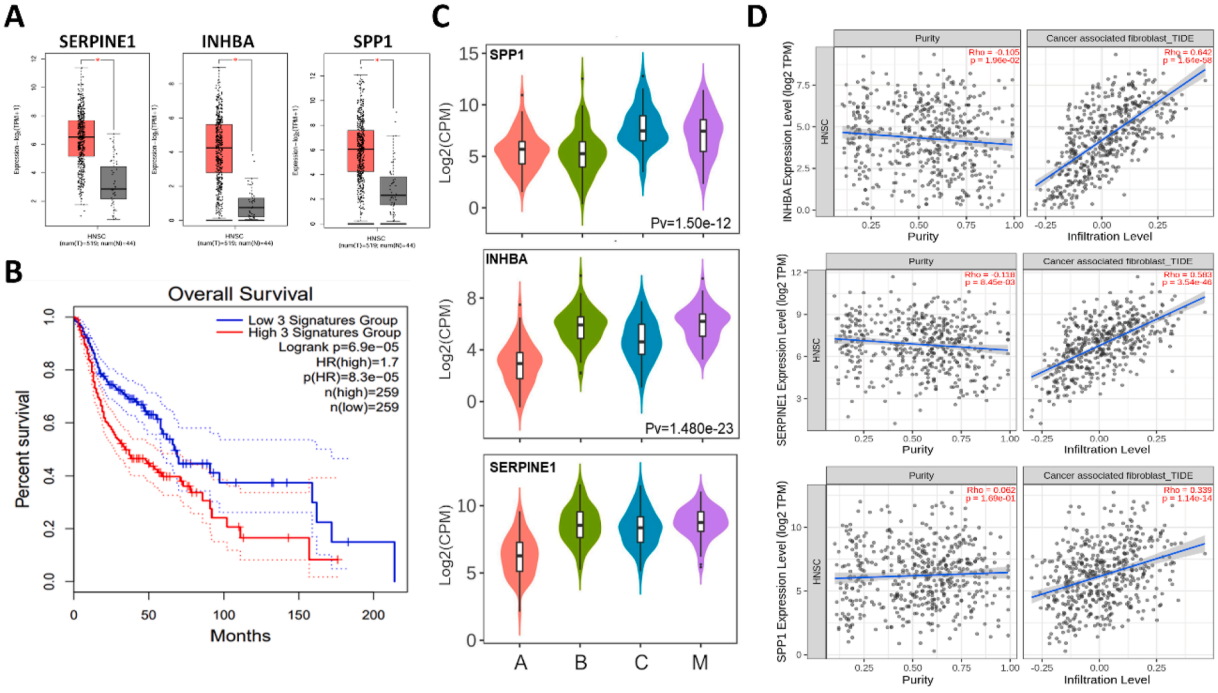

Figure 2 Elevated SERPINE1, INHBA, and SPP1 (SIS oncogenic signature) expression correlates with poor prognosis and high cancer-associated fibroblast infiltration in head and neck squamous cell carcinoma. (A) Box plots showing significantly higher mRNA expression of SERPINE1, INHBA, and SPP1 in tumor tissues compared to normal tissues from the TCGA database. (B) Kaplan–Meier survival curve demonstrating lower overall survival in patients with high SIS signature expression (hazard ratio = 1.7; log-rank P = 6.9e-05). (C) Expression profiles of SIS signature genes across different molecular subtypes (basal, classical, mesenchymal) of head and neck cancer. (D) Correlation analysis from TIMER 2.0 showing significant positive correlation between SIS signature expression and cancer-associated fibroblast infiltration (INHBA: Rho = 0.642, P = 1.64e-58; SERPINE1: Rho = 0.583, P = 3.54e-46; SPP1: Rho = 0.339, P = 1.14e-14). TCGA: The Cancer Genome Atlas; SIS: SERPINE1, INHBA, SPP1; TIMER: Tumor Immune Estimation Resource.

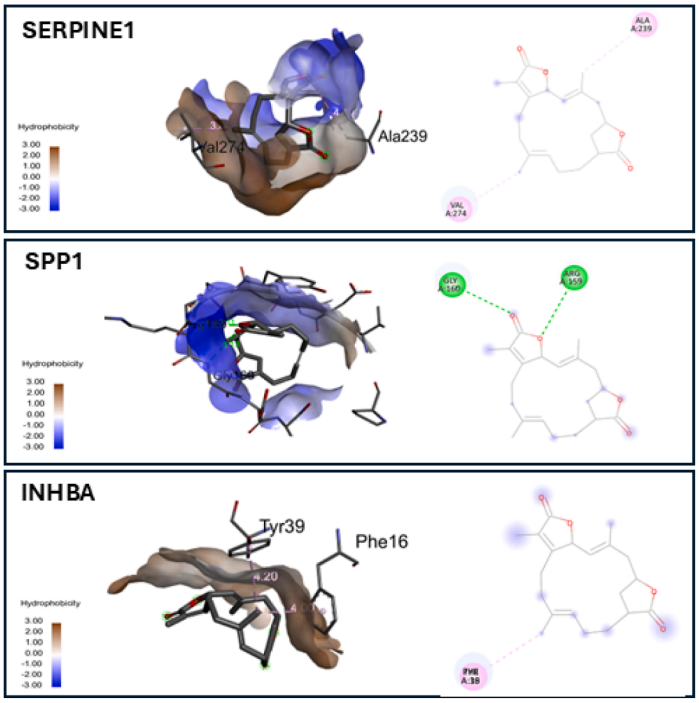

SERPINE1:Ovatodiolide (ΔG: **-7.5 kcal/mol**)

Amino Acid Position	Bond Interaction	Distance (Å)
Alanine 239	Alkyl	4.10
Valine 274	Alkyl	3.81

SPP1:Ovatodiolide (ΔG: **-6.5 kcal/mol**)

Amino Acid Position	Bond Interaction	Distance (Å)
Arginine 159	Conventional H Bond	3.11
Glycine 160	Conventional H Bond	3.13

INHBA:Ovatodiolide (ΔG: **-6.4 kcal/mol**)

Amino Acid Position	Bond Interaction	Distance (Å)
Phenylalanine 16	Pi-Alkyl	4.00
Tyrosine 39	Pi-Alkyl	4.20

Figure 3 Molecular docking simulations of ovatodiolide and the SIS oncogenic signature. The three-dimensional (left) and two-dimensional (right) views of the lowest-energy docking poses of ovatodiolide bound to SERPINE1 (upper panel, $\Delta G = -7.5$ kcal/mol), SPP1 (middle panel, $\Delta G = -6.5$ kcal/mol), and INHBA (lower panel, $\Delta G = -6.4$ kcal/mol). Hydrophobic surfaces are shown in brown (scale: -3 to $+3$), while polar regions are represented in blue. Key interacting residues and bond types are indicated: hydrogen bonds (green dashed lines), $\pi-\pi$ stacking (purple dashed line), and van der Waals contacts. Ovatodiolide exhibits the strongest predicted affinity for SERPINE1, followed by SPP1 and INHBA.

flanking hydrophobic side chains (Ile237, Phe358, Ala238) stabilize the orientation (middle panel, Fig. 3). In the INHBA docking pose, a combination of $\pi-\pi$ stacking with Phe16 and hydrogen bonding to Tyr39 within a hydrophobic L3—α1 crevice underpins complex formation (lower panel, Fig. 3). Collectively, these data provide a structural rationale for ovatodiolide as a multitarget disruptor of the SIS oncogenic signature.

Cancer-associated fibroblast coculture promotes SERPINE1, INHBA, and SPP1 expression and cisplatin resistance

Next, we performed in vitro experiments using HNSCC cell lines to validate our bioinformatics results. A cell viability assay yielded IC50 values for cisplatin in CAL27 and Ca9-22 cells (Fig. 4A). We then generated HNSCC tumor spheroids to mimic cancer stem-like cells. The tumor spheroids demonstrated significantly higher IC50 values for cisplatin, reflecting their inherent drug resistance (Fig. 4B). Subsequently, we examined the effects of tumor cells on the TME by collecting the tumor culture medium (termed tumor-conditional medium, TCM) and culturing WS1 (normal fibroblasts). TCM-treated WS1 cells were transformed into cancer-associated fibroblasts (CAFs), as indicated by their increased expression of α-SMA, vimentin (Vim), and TGFβ1 (Fig. 4C). In a parallel experiment, CAF-conditional medium (CAF-CM) was used to culture the parental CAL27 and Ca9-22 cells. CAF-CM-treated tumor cells exhibited an enhanced ability to generate tumor spheroids under serum-free 3D culture conditions (Fig. 4D). Furthermore, tumor spheroids generated from CAF-CM express significantly higher levels of the SIS oncogenic signature, markers of metastasis (MMP1 and 3), and cancer stemness (CD44 and YAP1) (Fig. 4E). These observations support the SIS oncogenic signature in promoting cancer stemness and drug resistance.

Ovatodiolide suppresses cancer stemness and reduces CAF transformation

According to our molecular docking simulations, ovatodiolide can form a stable complex with the members of the SIS oncogenic signature. Therefore, it prompts us to examine its potential as an anti-HNSCC agent. HNSCC cells were treated with ovatodiolide, demonstrating their sensitivity (Fig. 5A). Comparative qPCR and Western blot analyses revealed that ovatodiolide treatment reduced the expression of the SIS oncogenic signature, metastatic markers (MMP1 and 3), and stemness markers (CD44 and YAP1, Fig. 5B). In support, ovatodiolide-treated HNSCC cells exhibited a significantly reduced spheroid-forming ability, echoing the decreased expression in CD44 and YAP1 (Fig. 5C). Subsequently, we examined ovatodiolide's effects on CAF transformation by culturing WS1 cells with tumor-conditional medium (TCM) and ovatodiolide-treated

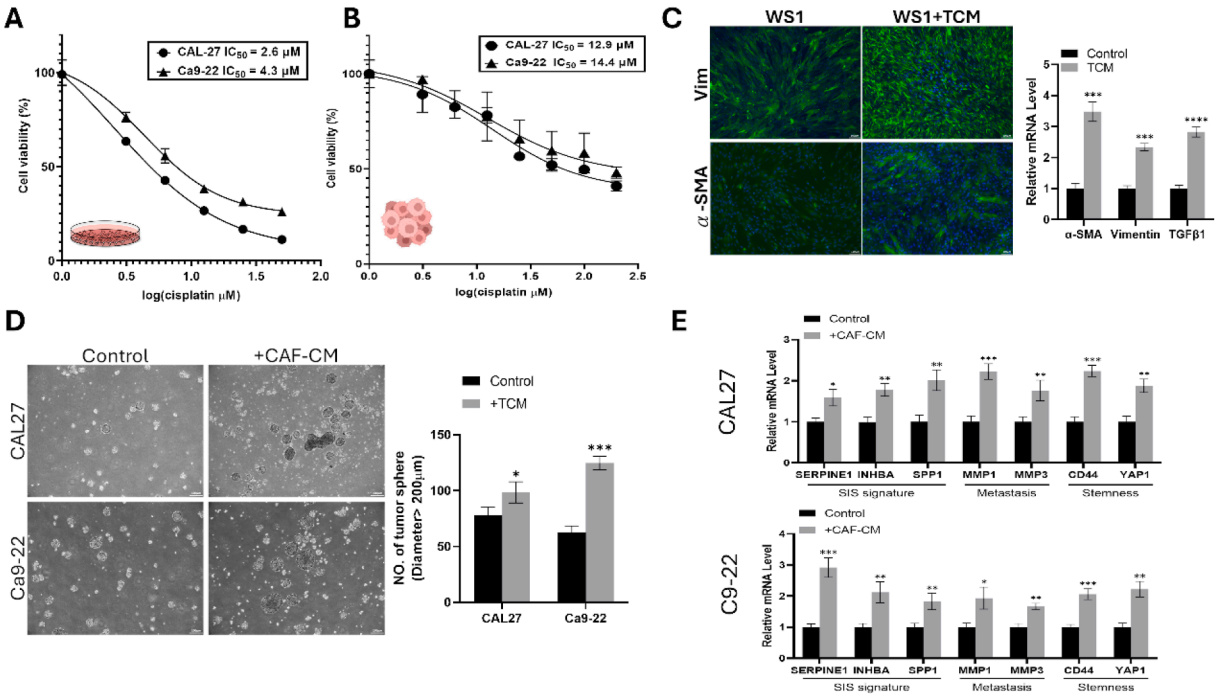

Figure 4 Cancer-associated fibroblasts-derived signals enhance chemoresistance, stemness, and metastatic potential in tumor cells. Dose-response curves illustrate the effect of cisplatin on the viability of CAL-27 and Ca9-22 HNSCC cells (A) and tumor spheroids (B). IC50 values are indicated. (C) Transformation of cancer-associated fibroblast (CAF)-like phenotype in WS1 fibroblasts by tumor-conditional medium (TCM). Immunofluorescence staining for vimentin (Vim) and α-smooth muscle actin (α-SMA) is shown. Right panel: Quantitative RT-PCR analysis of α-SMA, Vim, and TGFB1 mRNA expression in WS1 cells treated with TCM versus control. (D) Representative images (left) and quantification (right) of spheroid formation by CAL-27 and Ca9-22 cells cultured in control medium or CAF-conditioned medium (CAF-CM). Only spheroids with a diameter of >200 μm were tabulated. (E) qPCR analysis of tumor spheroids generated under control and CAF-CM conditions. Relative mRNA expression of the SIS signature (SERPINE1, INHBA, SPP1), metastasis (MMP1, MMP3), and stemness (CD44, YAP1) in HNSCC spheroids generated from control medium or CAF-CM, as determined by quantitative RT-PCR. TCM, tumor-conditional medium. CAF-CM, cancer-associated fibroblast conditioned medium. ***$P < 0.001$.

tumor-conditional medium (Ovato-TCM). WS1 cells cultured with Ovato-TCM displayed significantly lower expression of a-SMA, Vim, and TGFB1 (CAF markers) than their control counterparts (Fig. 5C), suggesting that adding ovatodiolide prevented CAF transformation. Collectively, these findings indicate that ovatodiolide suppresses HNSCC tumorigenesis by reducing the SIS oncogenic signature and CAF transformation.

Ovatodiolide treatment delays tumorigenesis in vivo and overcomes cisplatin resistance

To validate our bioinformatics and in vitro results, we utilized a Ca9-22 tumoroid (containing CAFs)-bearing xenograft mouse model to assess the therapeutic potential of ovatodiolide. The tumor size over time curves demonstrated that Ca9-22 tumors were resistant to cisplatin, as there was no significant difference between the tumor growth curves of the sham and cisplatin-alone groups (Fig. 6A). Mice that received ovatodiolide exhibited significantly delayed tumor growth compared to their sham and cisplatin-alone counterparts (Fig. 6A). Notably, the combination regimen of ovatodiolide and cisplatin, where cisplatin was administered at half the dose used in the monotherapy group (2.5 mg/kg), resulted in the most pronounced delay of tumor growth, suggesting that ovatodiolide effectively re-sensitizes these cisplatin-resistant tumoroids to cisplatin (Fig. 6A). These findings were further corroborated by examining the tumor weights at the study endpoint, where tumors harvested from the ovatodiolide only and combination treatment groups were significantly smaller than those from the sham and cisplatin-alone groups (Fig. 6B). Additionally, we showed that the spheroid-forming ability was markedly reduced by ovatodiolide alone and the combination treatment, compared to the sham and cisplatin-alone counterparts (Fig. 6C). Quantitative PCR analysis of the tumor samples revealed that the elevated expression of the SIS signature (SERPINE1, INHBA, SPP1), was significantly suppressed by ovatodiolide and the combination regimen, but not by cisplatin alone (Fig. 6D). Furthermore, the expression of cancer stemness markers (YAP1, CD44) and the CAF marker FAP were significantly downregulated in tumors from the ovatodiolide and ovatodiolide + cisplatin combination groups (Fig. 6D). Aligns with the relative mRNA levels, the protein expression levels of SIS oncogenic signatures were decreased in ovatodiolide treatment groups alone and in combination with cisplatin (Fig. 6E). These in vivo data collectively demonstrated the therapeutic potential of ovatodiolide in

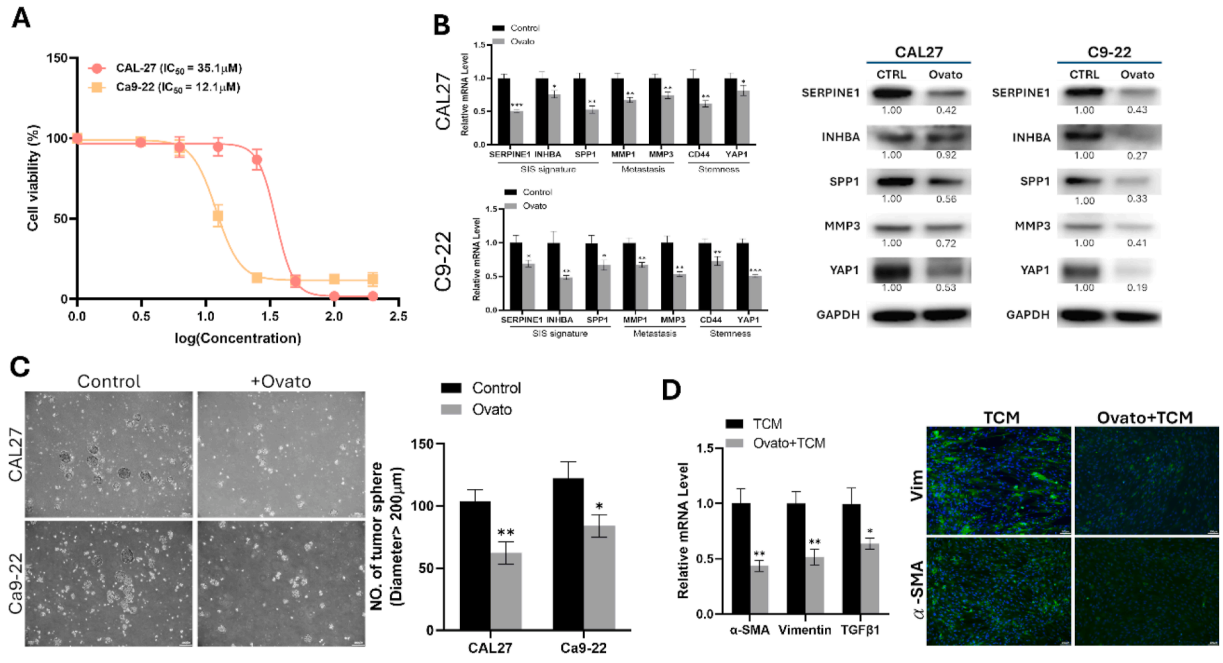

Figure 5 Ovatodiolide treatment reduces tumorigenesis, cancer stemness, and cancer-associated fibroblast transformation. (A) Dose-response curves showing ovatodiolide cytotoxicity in CAL27 and Ca9-22 cells (48 h). IC50 values are indicated in the box. (B) qPCR and Western blot analysis of SIS oncogenic signature genes (SERPINE1, INHBA, SPP1, MMP3, YAP1) in ovatodiolide-treated CAL27 and Ca9-22 cells. GAPDH served as a loading control. (C) Sphere formation assay showing reduced stemness after ovatodiolide treatment. Left: representative images of spheroids. Right: quantification of sphere numbers. Scale bar = 200 μm. (D) CAF transformation analysis. Left: Western blot of CAF markers (α-SMA, vimentin, TGF-β1) in WS1 fibroblasts treated with tumor-conditional medium (TCM) or ovatodiolide-treated TCM (Ovato + TCM). Right: Green immunofluorescence of α-SMA and vimentin. Scale bar = 50 μm *$P < 0.05$, **$P < 0.01$.

delaying HNSCC growth, overcoming cisplatin resistance, and targeting both cancer stemness and the CAF generation, consistent with our in vitro findings.

Discussion

Head and neck squamous cell carcinoma (HNSCC) remains a clinical challenge to manage, exhibiting high recurrence rates (therapy failure) and poor survival outcomes.[26,27] These issues are often linked to the complex crosstalk among tumor cells and the cellular components of the tumor microenvironment (TME).[28] Our study addresses these issues by identifying a novel, functionally cohesive oncogenic signature called SIS (SERPINE1, INHBA, and SPP1). This signature not only predicts poor prognosis and increased cancer-associated fibroblast (CAF) infiltration across HNSCC subtypes, but it also serves as a therapeutic target. We demonstrate that the SIS oncogenic network can be pharmacologically disrupted by ovatodiolide, a phytochemical that dampens the signaling between tumor cells and their TME by inhibiting cancer stemness and CAF transformation, thus providing a novel and dual-pronged approach to treating drug-resistant HNSCC.

Our initial transcriptomic analysis across three independent HNSCC datasets (GSE31056, GSE23558, GSE75538) yielded a consistent upregulation of nine genes (MMP1, MMP3, MMP10, SPP1, INHBA, SERPINE1, IL24, CXCL10, and SCG5) in tumor tissues compared to their normal counterparts. Subsequent network and pathway analyses revealed that a core subset of these genes, SERPINE1, MMPs, SPP1, and INHBA, forms a functional cluster significantly associated with the inflammatory and profibrotic pathways, matrix remodeling, and pivotal signaling cascades such as TGF-β and Oncostatin M signaling, which are essential to TME-driven HNSCC progression. From this, we distilled the SIS oncogenic signature (SERPINE1, INHBA, SPP1), selected for their established individual roles in tumorigenesis and TME modulation, as well as their collective power as a prognostic and mechanistic indicator. For instance, elevated SERPINE1 expression is associated with distant metastasis and cisplatin resistance in HNSCC patients.[29,30] Increased INHBA expression (a subunit of activin A) has been reported to drive EMT and metastasis, and facilitate immune surveillance.[31] Upregulation of SPP1 is detected in undifferentiated HNSCC tumor cells; its expression is correlated with the late stage of HNSCC and invasion.[32] The reported functions of the members of the SIS signature agree with our bioinformatics results, where elevated expression of the SIS signature predicts significantly lower overall survival rate in HNSCC patients. More importantly, the elevated SIS signature is observed across different HNSCC molecular subtypes (basal, classical, mesenchymal), suggesting its broad relevance in HNSCC and a novel oncogenic signature for HNSCC.

Furthermore, the significant positive correlation between the SIS signature expression, especially INHBA, and

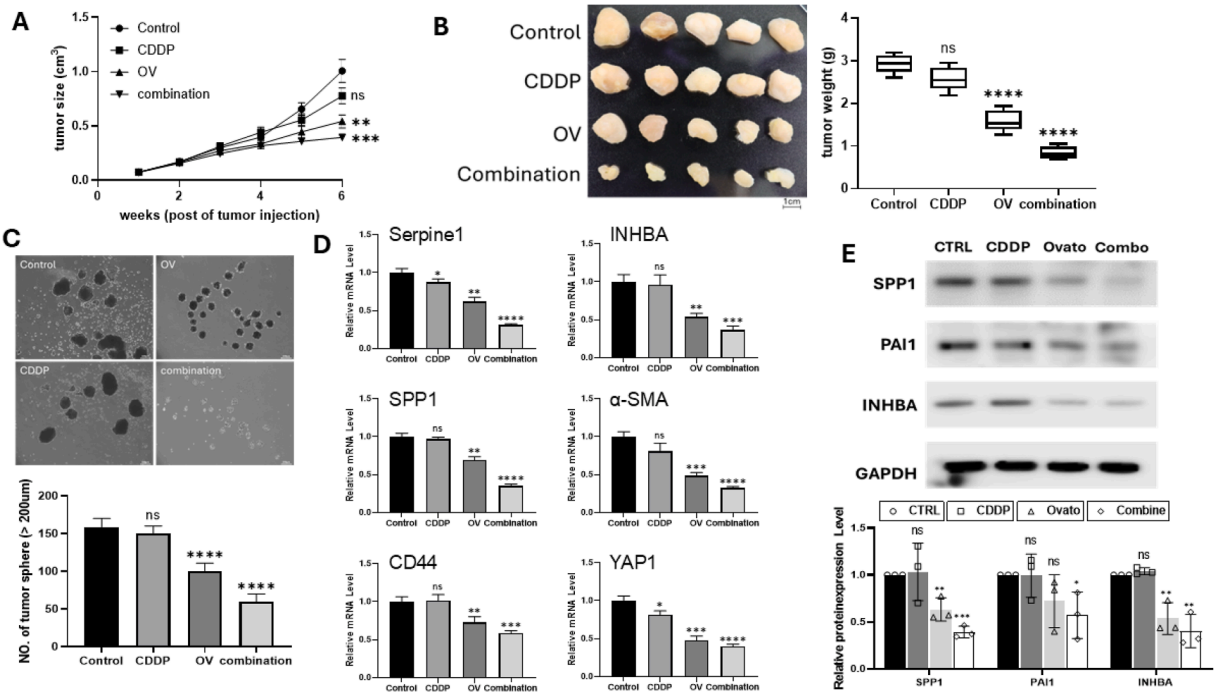

Figure 6 Ovatodiolide overcomes cisplatin resistance and delays HNSCC tumorigenesis in vivo. (A) Average tumor volume over time curves. Mice were randomly assigned to treatment groups: sham control, cisplatin, ovatodiolide, or a combination of CDDP + OV. Note that the sham control and cisplatin-only curves are not statistically different. (B) Photographs of harvested tumors from each treatment group at the experimental endpoint (left) and corresponding tumor weights (g) (right). Data are presented as box plots, showing the median and interquartile range, with whiskers extending to the minimum and maximum values. (C) Representative micrographs (upper panels) and quantification (bottom panel) of spheroid formation from dissociated tumor samples. Spheroids with a diameter ≥200 μm were calculated. (D) Relative mRNA expression levels of the SIS signature genes (SERPINE1, SPP1, INHBA), cancer stemness markers (CD44, YAP1), and the CAF marker FAP in harvested tumor samples from each treatment group, as determined by quantitative RT-PCR. mRNA levels are normalized to the control group. (E) Protein expression levels of SIS signature genes (SPP1, PAI1/SERPINE1, INHBA) of different treatment groups as determined by Western blot analysis. ns: not significant, *$P < 0.05$, **$P < 0.01$, ***$P < 0.001$. ****$P \leq 0.0001$. OV or Ovato, ovatodiolide. CDDP, cis-Diammineplatinum (II) dichloride.

the tumor-infiltrating level of cancer-associated fibroblasts (CAFs) signifies this signature's function of linking the tumor cells and the TME. CAFs are known to be a key cellular component of the pro-tumorigenic TME, not only promoting cancer cell proliferation, but also metastasis and drug resistance.[33] The strong association between the SIS signature and CAF infiltration suggests a reciprocal signaling loop in which tumor cells expressing the SIS signature actively recruit and activate fibroblasts (transformed to CAFs), facilitating tumorigenesis. Our in vitro experiments provided evidence supporting the notion that tumor-conditional medium (TCM) from HNSCC cells transformed normal fibroblasts into CAFs, characterized by increased expression of α-SMA, vimentin, and TGFB1. Conversely, CAF-conditioned medium (CAF-CM) enhanced the spheroid-forming ability (a surrogate of cancer stemness) of HNSCC cells, which was associated with the upregulation of the SIS signature, metastasis markers (MMP1/3), and stemness markers (CD44, YAP1) in these spheroids. These results validate the importance of the SIS-CAF axis, emphasizing how CAF-derived signals reinforce cancer stemness and cisplatin resistance.

After identifying the central role of the SIS signature and its association with CAFs, we investigated potential therapeutic strategies targeting SIS. Molecular docking simulations reveal that ovatodiolide, a natural macrocyclic diterpenoid with anti-inflammatory and anti-cancer activities reported in our previous studies,[9,25] is capable of forming stable complexes with the proteins of the SIS signature (SERPINE1, SPP1, and INHBA). Our subsequent in vitro experiments validated that ovatodiolide treatment suppressed HNSCC cell viability and reduced the expression of the SIS oncogenic signature, as well as metastasis markers (MMPs) and stemness markers (CD44 and YAP1). Consistently, ovatodiolide treatment significantly decreased the spheroid-forming capacity of HNSCC cells. Notably, ovatodiolide prevented the transformation of normal fibroblasts into cancer-associated fibroblasts (CAFs) induced by tumor-conditioned medium, as supported by the reduced expression of CAF markers (α-SMA, TGFB1, and Vimentin).

These findings suggest that ovatodiolide acts as a multitarget inhibitor, simultaneously disrupting the SIS oncogenic signature in tumor cells and interfering with the pro-tumorigenic activation of CAFs. This dual-targeting approach exhibits promise for partially normalizing the dysfunctional tumor microenvironment. Our in vitro data were supported by in vivo evidence, where ovatodiolide

treatment significantly delayed tumor growth in Ca9-22 tumoroid-bearing mice. More importantly, combining ovatodiolide and cisplatin treatment resulted in the slowest tumor growth rate, suggesting that ovatodiolide can overcome cisplatin resistance in the CAF-containing Ca9-22 tumoroids.

This finding aligns with previous studies using CAL27 and SAS xenograft mice models.[9,34] In both models, ovatodiolide as a single treatment and in combination with cisplatin was found to significantly inhibit tumor growth, indicated by a reduction in tumor size.[9,34] Moreover, in the CAL27 xenograft mouse model, ovatodiolide alone or in combination with cisplatin also significantly reduced tumor spheroid formation.[9]

Collectively, our study identifies the SIS oncogenic signature (SERPINE1, INHBA, SPP1) as a clinically relevant marker associated with poor prognosis and CAF infiltration in HNSCC. We provide functional evidence supporting a positive feedback loop between HNSCC cells and CAFs, wherein tumor-derived signals promote the transformation of CAFs. CAF-derived factors enhance HNSCC stemness and SIS signature expression, contributing to chemoresistance. Ovatodiolide is identified as a potential therapeutic agent capable of disrupting this SIS-CAF interaction by down-regulating SIS signature expression and preventing CAF transformation.

Although our study provides valuable insights, several limitations should be acknowledged. The clinical correlations of the SIS signature are based on publicly available datasets, so prospective studies are required to validate these findings. Our in vitro experimental results provide evidence for the tumorigenic role of the SIS signature within the HNSCC cells and the CAF-transforming function. However, these in vitro findings do not comprehensively recapitulate the complexity of the tumor microenvironment, which contains a spectrum of immune cells and other stromal components. Further mechanistic studies are necessary to elucidate how ovatodiolide interacts with SERPINE1, INHBA, and SPP1, as well as the precise signaling pathways involved in suppressing CAF transformation. Finally, a more nuanced pharmacokinetics and pharmacodynamics (PK/PD) study should be conducted to provide more foundation for future human trials.

Declaration of competing interest

All authors declare that they have no competing interests relevant to this article.

Acknowledgements

This study is funded by the New Investigator Grant from Taipei Medical University (TMU112-AE1-B27) and the Wan-Fang Hospital/Lotung Pohai Hospital joint research grant (11409/114-wf-pah-03), awarded to Kuan-Chou Lin. Jia-Hong Chen and Jih-Chin Lee are supported by the research grants from the Tri-Service General Hospital (TSGH_D_114076, TSGH_D_114072, respectively).

References

1. Asarkar AA, Flores JM, Nathan CAO. Comparison of survival estimates following recurrence, persistence, or second primary malignancy in oropharyngeal squamous cell carcinoma. *Otolaryngology* 2020;163:1209—17.
2. Lawrence MS, Sougnez C, Lichtenstein L, et al. Comprehensive genomic characterization of head and neck squamous cell carcinomas. *Nature* 2015;517:576—82.
3. Choonoo G, Blucher A, Higgins S, et al. Illuminating biological pathways for drug targeting in head and neck squamous cell carcinoma. *PLoS One* 2019;14:e0223639.
4. Elhanani O, Ben-Uri R, Keren L. Spatial profiling technologies illuminate the tumor microenvironment. *Cancer Cell* 2023;41:404—20.
5. Jin MZ, Jin WL. The updated landscape of tumor microenvironment and drug repurposing. *Signal Transduct Targeted Ther* 2020;5:166.
6. Reis PP, Waldron L, Perez-Ordonez B, et al. A gene signature in histologically normal surgical margins is predictive of oral carcinoma recurrence. *BMC Cancer* 2011;11:437.
7. Ambatipudi S, Gerstung M, Pandey M, et al. Genome-wide expression and copy number analysis identifies driver genes in gingivobuccal cancers. *Genes Chromosomes Cancer* 2012;51:161—73.
8. Krishnan NM, Dhas K, Nair J, et al. A minimal DNA methylation signature in oral tongue squamous cell carcinoma links altered methylation with tumor attributes. *Mol Cancer Res* 2016;14:805—19.
9. Chen JH, Wu ATH, Bamodu OA, et al. Ovatodiolide suppresses oral cancer malignancy by down-regulating exosomal mir-21/stat3/β-catenin cargo and preventing oncogenic transformation of normal gingival fibroblasts. *Cancers (Basel)* 2019;12:56.
10. Chen JH, Wu ATH, Lawal B, et al. Identification of cancer hub gene signatures associated with immune-suppressive tumor microenvironment and ovatodiolide as a potential cancer immunotherapeutic agent. *Cancers (Basel)* 2021;13:1234.
11. Barrett T, Wilhite SE, Ledoux P, et al. Ncbi geo: archive for functional genomics data sets—update. *Nucleic Acids Res* 2013;41:D991—5.
12. Bardou P, Mariette J, Escudie F, et al. Jvenn: an interactive venn diagram viewer. *BMC Bioinf* 2014;15:293.
13. Szklarczyk D, Kirsch R, Koutrouli M, et al. The string database in 2023: Protein—protein association networks and functional enrichment analyses for any sequenced genome of interest. *Nucleic Acids Res* 2023;51:D638—46.
14. Tang Z, Kang B, Li C, et al. Gepia2: an enhanced web server for large-scale expression profiling and interactive analysis. *Nucleic Acids Res* 2019;47:W556—60.
15. Ru B, Wong CN, Tong Y, et al. Tisidb: an integrated repository portal for tumor-immune system interactions. *Bioinformatics* 2019;35:4200—2.
16. Li T, Fu J, Zeng Z, et al. Timer 2.0 for analysis of tumor-infiltrating immune cells. *Nucleic Acids Res* 2020;48:W509—14.
17. Harrington AE, Morris-Triggs SA, Ruotolo BT, et al. Structural basis for the inhibition of activin signalling by follistatin. *EMBO J* 2006;25:1035—45.
18. UniProt C. Uniprot: the universal protein knowledgebase in 2025. *Nucleic Acids Res* 2025;53:D609—17.
19. Waterhouse A, Bertoni M, Bienert S, et al. Swiss-model: homology modelling of protein structures and complexes. *Nucleic Acids Res* 2018;46:W296—303.
20. Eberhardt J, Santos-Martins D, Tillack AF, et al. Autodock vina 1.2.0: new docking methods, expanded force field, and python bindings. *J Chem Inf Model* 2021;61:3891—8.

21. Wu ATH, Yeh YC, Huang YJ, et al. Gamma-mangostin isolated from garcinia mangostana suppresses colon carcinogenesis and stemness by downregulating the gsk3β/β-catenin/cdk6 cancer stem pathway. *Phytomedicine* 2022;95:153797.
22. Chen S, Li Y, Zhu Y, et al. Serpine1 overexpression promotes malignant progression and poor prognosis of gastric cancer. *J Oncol* 2022;2022:2647825.
23. Pavon MA, Arroyo-Solera I, Cespedes MV, et al. Upa/upar and serpine1 in head and neck cancer: role in tumor resistance, metastasis, prognosis and therapy. *Oncotarget* 2016;7: 57351—66.
24. Yu Z, Cheng L, Liu X, et al. Increased expression of inhba is correlated with poor prognosis and high immune infiltrating level in breast cancer. *Front Bioinform* 2022;2:729902.
25. Huang YJ, Yang CK, Wei PL, et al. Ovatodiolide suppresses colon tumorigenesis and prevents polarization of m2 tumor-associated macrophages through yap oncogenic pathways. *J Hematol Oncol* 2017;10:60.
26. Schutte HW, Heutink F, Wellenstein DJ, et al. Impact of time to diagnosis and treatment in head and neck cancer: a systematic review. *Otolaryngology* 2020;162:446—57.
27. Zhang A, Jin Y, Zou X, et al. Molecular subtyping and prognostic risk characterization of head and neck squamous cell carcinoma based on lysosome-related genes. *Medicine* 2023;102: e34275.
28. Chen SMY, Krinsky AL, Woolaver RA, et al. Tumor immune microenvironment in head and neck cancers. *Mol Carcinog* 2020;59:766—74.
29. Guo X, Sun Z, Chen H, et al. Serpine1 as an independent prognostic marker and therapeutic target for nicotine-related oral carcinoma. *Clin Exp Otorhinolaryngol* 2023;16:75—86.
30. Pavón MA, Arroyo-Solera I, Téllez-Gabriel M, et al. Enhanced cell migration and apoptosis resistance may underlie the association between high serpine1 expression and poor outcome in head and neck carcinoma patients. *Oncotarget* 2015;6: 29016—33.
31. De Martino M, Daviaud C, Vanpouille-Box C. Activin a backs-up tgf-ß to promote regulatory t cells. *OncoImmunology* 2021;10: 1883288.
32. Bie T, Zhang X. Higher expression of spp1 predicts poorer survival outcomes in head and neck cancer. *J Immunol Res* 2021;2021:8569575.
33. Kanzaki R, Pietras K. Heterogeneity of cancer-associated fibroblasts: opportunities for precision medicine. *Cancer Sci* 2020;111:2708—17.
34. Lin CS, Bamodu OA, Kuo KT, et al. Investigation of ovatodiolide, a macrocyclic diterpenoid, as a potential inhibitor of oral cancer stem-like cells properties via the inhibition of the jak2/stat3/jarid1b signal circuit. *Phytomedicine* 2018;46: 93—103.